"Nose-like" structures in the inner magnetosphere: Comparing RCM simulations with Cluster observations

J.-C. Zhang[1](jichun.zhang@unh.edu), L. M. Kistler[1], R. A. Wolf[2], H. Matsui[1], C. G. Mouikis[1], S. Sazykin[2], I. Dandouras[3, 4], and B. Klecker[5]

[1]Space Science Center, University of New Hampshire, Durham, NH 03824, USA
[2]Department of Physics and Astronomy, Rice University, Houston, TX 77005, USA
[3]Université de Toulouse, Centre d'Etude Spatiale des Rayonnements, Toulouse, France
[4]CNRS, UMR 5187, Toulouse, France [5]Max-Planck-Institut für extraterrestrische Physik, Garching, Germany

2011 CEDAR-GEM Joint Summer Workshop, Santa Fe, NM, June 26 – July 1, 2011

Paper#: 31

Abstract

Ion "nose-like" structures, often observed by spacecraft in the inner magnetosphere, are due to the single or combined effect of several factors on ion access to the inner magnetosphere: convection, corotation, gradient and curvature drifts, losses, and changes in the convection electric field and/or the ion source population. Several different mechanisms have been suggested as being involved in the formation of nose structures, but it is not clear which is the dominant one or how they all combine to produce the observed phenomena. In this study, we report our initial results of the Rice Convection Model (RCM) simulations of the nose structures detected by Cluster on 18 May 2004 (single-nose) and 11 April 2002 (multiple-nose). It is indicated that combining RCM simulations and Cluster observations to investigate nose structures can provide new insight into the physics of inner-magnetospheric ion access and into the limitations of the theories and modeling of the inner magnetosphere.

What Are Nose Structures?

1. Named after "nose-like" features in the energy-time spectrograms of *in-situ* measured ion fluxes in the inner magnetosphere [e.g., *Smith & Hoffman*, 1974; *Vallat* et al., 2007; *Dandouras et al.*, 2009]

2. Still a significant outstanding issue in Space Physics because of the critical but unanswered questions concerning them, e.g., the dominant mechanism of their formation

3. Constitute a test ground for the inner-magnetospheric theories and modeling

Motivation

1. How do ions access the inner magnetosphere, and what is the role of nose structures in the injection process?

2. What factors control injection and nose structures?

3. How well does RCM, one of the best inner-magnetospheric models, reproduce nose structures?

RCM & Its Setup

* RCM Code: self-consistently compute particle drifts, electric currents, & electric fields to describe the motion of plasma in the inner & middle magnetosphere, w/ prescribed magnetic fields
* Initial Condition: empty magnetosphere, run for 12 hours before realistic inputs are applied
* Inputs: 5-min OMNI solar wind number density, bulk flow speed, IMF B_z, polar cap potential drop, and *Dst*
* Magnetic Field: T96 [*Tsyganenko & Stern*, 1996]
* Tailward Plasma Boundary: an empirical plasma-sheet model [*Tsyganenko & Mukai*, 2003]
* Ion Composition: a *Kp*- & *F10.7*-based formula [*Young et al.*, 1982]
* Internal Ion Losses (i.e., Charge Exchange): not applied

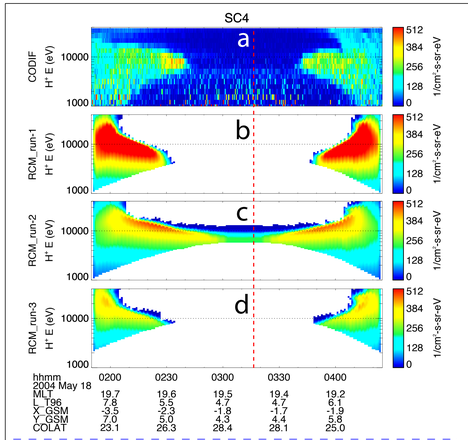

Fig. 1: SC4/CIS-CODIF data (Panel a) vs. RCM simulation results from three runs (Panel b: standard, Panel c: halved plasma-sheet *N*, & Panel d: doubled plasma-sheet *T*) during the perigee pass of the spacecraft (the vertical dashed line)

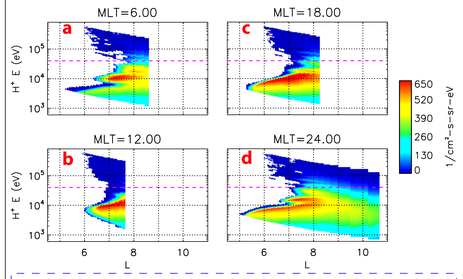

Fig. 2: RCM simulated H^+ spectrograms at four magnetic local times, MLT = 06 (a), 12 (b), 18 (c), and 24 (d), at 06:00 UT on 18 May 2002 in the standard run (Fig. 1b).

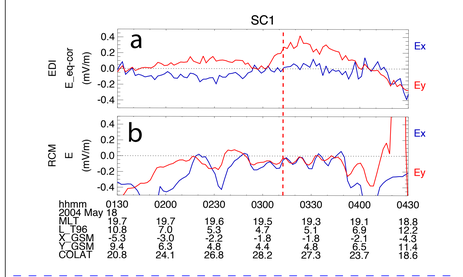

Fig. 3: Electric field comparisons between RCM simulation results (Panel b) and SC1/EDI measurements (Panel a), which have been mapped to the magnetic equatorial plane and corotation has been subtracted from. RCM results are from the standard run (Fig. 1b).

Single Noses on 18 May 2004

Fig. 1:

❖ Panel a [Cluster Data]: The H^+ structure observed on the inbound pass is a single nose, but a second flux-enhanced structure appears at higher energies on the outbound pass, indicating a second nose that probably exceeds the energy limit (≤ 40 keV) of the CODIF instrument.

❖ Panel b [Standard RCM Run]: Noses on both the inbound & outbound passes are fairly well reproduced by RCM. However, the fluxes in the simulated noses are clearly higher than observations and the tips of the noses do not extend to low enough L values.

❖ Panel c [RCM Run with Halved Boundary *N*]: Flux values become even more comparable to the Cluster data and H^+ penetrate onto much lower L-shells (obviously too low).

❖ Panel d [RCM Run with Doubled Boundary *T*]: Though not affecting the depth of the nose tips, the higher temperature reduces the simulated fluxes significantly and increases the energy of the nose tips.

Fig. 2:

❁ As a large-scale magnetospheric model, RCM can provide a more complete picture of the nose structures than the observations themselves could provide.

❁ The energy increase along the decreasing L in the discrete-energy bands above the CODIF energy upper limit, i.e., 40 keV (the dashed lines), is due to the Betatron-Fermi acceleration when H^+ adiabatically drift to lower L-shells.

❁ It is surprising that some fine structures, overlapping the bigger and deeper nose structure, exist at all the four local times. In a test run in which the RCM solar wind inputs are fixed at 01:00 UT, all those fine structures disappear but the big nose is still there (not shown).

Fig. 3:

❁ Large data-model discrepancies in the beginning and end of the plot period are due to unreliable calculations near the RCM outer boundary.

❁ The EDI E_y enhancement around 03:22 UT is likely associated with mild substorm activity, in which the AE index was elevated up to 209 nT . The substorm might also have been the cause of the second nose on the outbound perigee pass of SC4 (Fig. 1a). Note that the RCM run does not include the substorm activity.

Multiple Noses on 11 April 2002

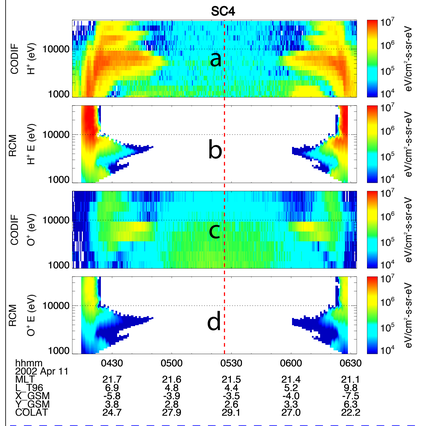

Fig. 4: SC4/CIS-CODIF (Panels a & c) vs. RCM (Panels b & d) for H^+ and O^+, respectively, on the perigee pass (the vertical line)

Fig. 4:

❁ Panel a: Triple noses were detected on both the inbound & outbound passes, when AE ≤ 75 nT.

❁ Panel c: Low CODIF energy-resolution for O^+ makes the multiple O^+ noses less distinct, especially the second & third noses.

❁ Panels b & d: The second & third noses are not reproduced, though there is a weak secondary nose at lower energies. But, fine structures similar to Fig. 2 are also present in this RCM run.

Summary & Discussion

- Preliminary results indicate that RCM, a state-of-the-art self-consistent electric field model, is sophisticated enough to investigate the dominant formation process of nose structures.
- Ion density & temperature in the plasma sheet are two of the factors that control the formation and characteristics (e.g., min. L or depth, energy at the nose tip, and peak flux value) of nose structures, i.e., the access of ions to the inner magnetosphere.
- Fine structures over the single nose (Fig. 2) are caused by variations in RCM inputs, which in turn could result in ion drift echoes, i.e., high-energy ions drifting faster than low-energy ions so that their population is superposed on the slower one locally [*Li et al.*, 2000]. The relationship between the fine structures and multiple noses will be further examined.
- Using a boundary condition for substorm/bubble injection in RCM [e.g., *Zhang et al.*, 2009] might be a way to better reproduce EDI data and/or a multiple nose.
- We will continue to investigate nose structures with RCM by evaluating previously proposed nose formation mechanisms as well as those singled out from our Cluster-RCM comparisons.
- This type of study will be of benefit to upcoming NASA missions, particularly the Radiation Belt Storm Probes (RBSP). Better physical knowledge of ion access to the inner magnetosphere will be critical for interpreting the 2-point RBSP measurements.

References

Dandouras, I., et al. (2009), *JGR, 114*, A01S90.
Li, X. L., et al. (2000), *GRL, 27*, 10.
Smith, P. H., & R. A. Hoffman (1974), *JGR, 79*, 7.
Tsyganenko, N. A., & D. P. Stern (1996), *JGR, 101*, A12.
Tsyganenko, N. A., & T. Mukai (2003), *JGR, 108*, 1136.
Vallat, C., et al. (2007), *AG, 25*, 1.
Young, D. T., et al. (1982), *JGR, 87*, A11.
Zhang, J.-C., et al. (2009), *JGR, 114*, A08219.

Acknowledgements

Work at UNH was supported by NASA through grant NNX11AB65G and by the RBSP-ECT project. The authors thank the NSSDC OMNI Data Center and the Cluster team for making their data and/or software available.